frontiers
in Materials

Influence of Solidification Microstructure on Mechanical Properties of $Al_{0.8}CrCuFeNi_2$ High Entropy Alloy

Julien Zollinger[1,2]* and Eric Fleury[2,3]

[1] Department of Metallurgy & Materials Science and Engineering, Institut Jean Lamour, Université de Lorraine, Nancy, France,
[2] Laboratory of Excellence on Design of Alloy Metals for low-mAss Structures (DAMAS), Université de Lorraine, Metz, France,
[3] Université de Lorraine, CNRS, Arts et Métiers ParisTech, LEM3, Metz, France

The solidification microstructure of $Al_{0.8}CrCuFeNi_2$ high entropy alloy consists of primary fcc dendrites decorated with interdendritic bcc and B2 phases. In this work the mechanical properties obtained for columnar oriented growth and equiaxed microstructures are compared. Highest properties are obtained for columnar structures when loading is parallel to the growth direction due to confinement of the deformation inside the columnar dendrite trunks.

Keywords: solidification, high entropy alloys, mechanical properties, microstructure, multi-phase alloys

1. INTRODUCTION

High Entropy Alloys (HEAs) are equiatomic multicomponent alloys that form simple solid solutions without embrittling intermetallics compounds. Since the development of the HEAs concept (Cantor et al., 2004; Yeh et al., 2004), the probably most studied has been the CoCrFeMnNi alloy that exhibits a simple fcc crystal structure but very high mechanical properties down to cryogenic temperatures (Gludovatz et al., 2014). Many alloys are derived from it, replacing the problematic manganese and cobalt with other elements, such as copper, or increasing Ni of Fe content. Interestingly, alluminium additions allows to modify and tune the crystal structure from fcc to bcc (Tang et al., 2013). An increasing Al content in the alloy will change the fcc structure to a mixture of fcc and bcc, to a single bcc structure for higher additions, even in the as-cast state (Guo et al., 2013). Two-phase alloys are generally the most interesting owing to their superior mechanical properties that can be optimized by adjusting the volume fraction, size of dispersion of both phases.

In this work, a two-phases $Al_{0.8}CrCuFeNi_2$ alloy is investigated. This alloy starts to solidify with a fcc crystal structure, and due to microsegregation of alloying elements a bcc phase appears during solidification (Choudhuri et al., 2017). Under the usual casting conditions, the primary phase solidifies in the form of dendrites whose arms grow with the <100> directions parallel to the thermal gradient. When the thermal gradient is low enough, free growth can occur and lead to an equiaxed microstructure. The different mechanical properties resulting from these two types of microstructure is well-known since a long time in the field of Nickel-based superalloys (Versnyder and Shank, 1970) but has never been studied for HEAs. This paper shows the first results obtained for $Al_{0.8}CrCuFeNi_2$ alloy and with an emphasis on the effect of solidification microstructure anisotropy on the obtained microstructure and properties.
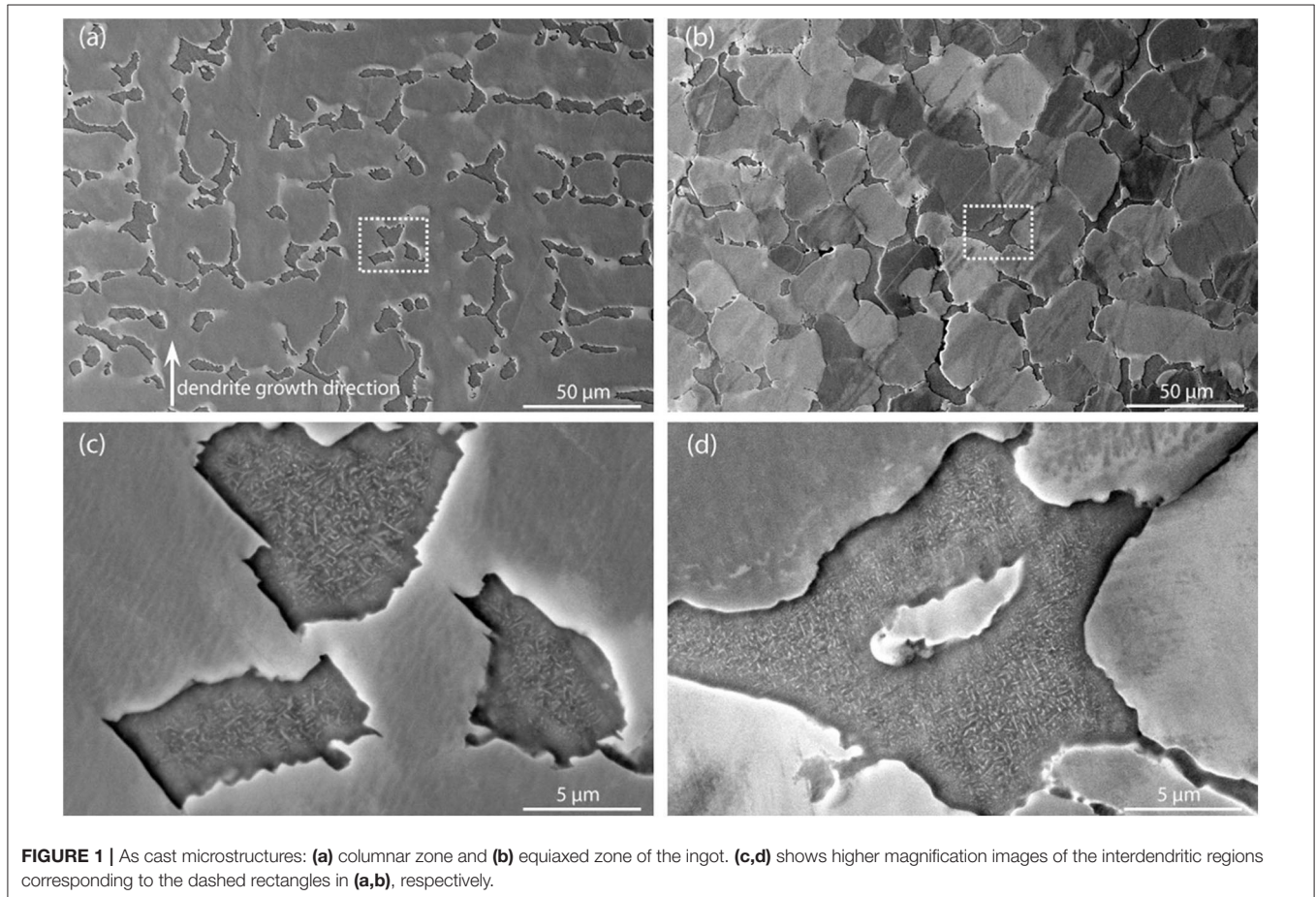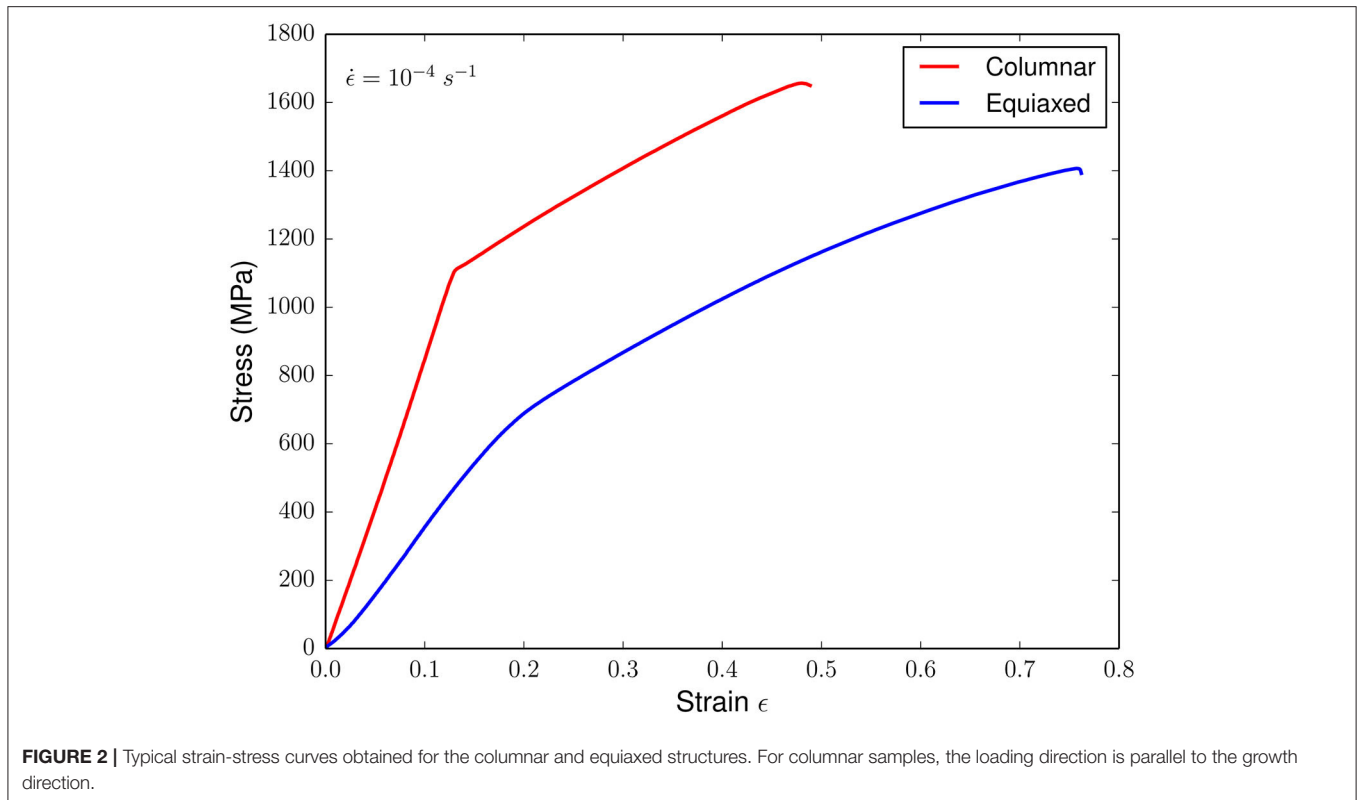
2. EXPERIMENTAL DETAILS

$Al_{0.8}CrCuFeNi_2$ alloys were prepared using a cold crucible induction melting furnace from commercial purity elements (>99.8%). Samples were cast using an Inducast tilt-caster into a cylindrical mold (20 mm diameter, 50 mm height) with alumina wall and a copper base, in order to achieve a directional solidification. With this set-up, the first 2 cm of alloy in contact with the copper shows a columnar zone while the top zone is fully equiaxed (see section 3). Three samples were prepared and cast, from which were machined $10 \times 10 \times 4$ mm^3 specimens for compression tests in both columnar and equiaxed zones. After standard metallographic preparation with colloidal silica finishing, SEM BSE images and EDS analyses were performed on a FEI Quanta 600 F FEG-SEM equipped with a Brücker Si-drift Quantax EDS detector. Samples were also examined by optical microscopy. Compression specimens were polished on one side prior to loading in order to observe the microstructure after deformation. Compression tests were made on a 50 kN MTS mechanical test system with a compression rate of 20 mm/min.

3. RESULTS AND DISCUSSION

Figure 1 shows the microstructure of the alloy at different locations and different magnifications. The columnar microstructure can be observed in **Figure 1a**, where the growth direction, parallel to the thermal gradient is indicated by the vertical arrow. It can be seen that the fcc phase primary arms, growing following the <100> direction in cubic metals are aligned with the thermal gradient. Dendrites are decorated with interdendritic secondary phases whose details are given in **Figure 1c**. While a single bcc phase was expected, some precipitates, visible in light gray on the BSE image and with typical size < 100 nm are also observed. This microstructure is similar to those observed by Guo et al. (2017) where the precipitates are identified as a Fe and Cr rich bcc phase while the interdendritic matrix consists of an Al and Ni rich B2 ordered structure. **Figure 1b** presents the microstructure observed in the equiaxed region, where the typical grain size is around 40 μm. Except for its morphology, the phases are the same as in the columnar zone, with fcc equiaxed grains decorated with a mixture of bcc and B2 phases as shown in **Figure 1d**. It is interesting to note that the primary arms spacing in the columnar zone and the grain size of the equiaxed region take very similar values. Since primary arm spacing depends on thermal gradient and interface velocity, and equiaxed grain size varies mainly with undercooling and number of potent nucleants, this is rather fortuitous but result in microstructures having similar characteristic lengths as well as secondary phases size and distribution. Moreover, the fraction of secondary

FIGURE 1 | As cast microstructures: **(a)** columnar zone and **(b)** equiaxed zone of the ingot. **(c,d)** shows higher magnification images of the interdendritic regions corresponding to the dashed rectangles in **(a,b)**, respectively.

FIGURE 2 | Typical strain-stress curves obtained for the columnar and equiaxed structures. For columnar samples, the loading direction is parallel to the growth direction.

TABLE 1 | Average values obtained from the compression and hardness tests (S.D., standard deviation deduced from the three specimens tested for each type of microstructure).

Microsctructure	Young Modulus E (GPa)	Y_s (MPa)	$R_{p0.2}$ (MPa)	R_m (Mpa)	Hardness (HV_{30})
Equiaxed	132	650	832	1,406	345
(S.D.)	(2)	(42)	(81)	(145)	(5)
Columnar	292	1,050	1,350	1,656	341
(S.D.)	(20)	(70)	(140)	(155)	(5)

phases, determined by image analysis and supplemented by microsegregation analyzes is also very close in the two types of microstructures, and are 20.7 ± 1.1 and $18.6 \pm 0.8\%$ for the columnar and equiaxed zone, respectively.

The uniaxial compression properties obtained for both columnar and equiaxed structures are presented in **Figure 2**, and values of the mechanical properties have been summarized in **Table 1**. For this two-phase alloy, the directionally solidified structure displayed superior mechanical properties in terms of Young's modulus, yield strength, and maximum compression strength in comparison to the equiaxed structure. In contrast the total plastic deformation accommodated by the alloy with directionally solidified structure is slightly reduced, while the work-hardening are found to be similar. The hardness takes similar values for both microstructure, and has been measured perpendicularly to the growth direction in the columnar sample. The crystallographic texture is less pronounced in this direction since directionally solidified alloys usually have a fiber type texture. This result shows that intrinsic phases

properties between the two types of microstructure are similar. For nickel-based superalloy, Versnyder and Shank (1970) reported superior values of the room temperature strength for directionally solidified structure in comparison to equiaxed structure. However, in comparison to nickel-based superalloy that are composed of two phases having similar lattice parameters and identical crystallographic orientation, the microstructure obtained in this directionally solidified alloy is more complex since the interdendritic region is misoriented in comparison to the dendrites. Indeed, the fcc and bcc/B2 phases formed during solidification are related through Kurdjumov-Sachs orientation relationships, as shown by Borkar et al. (2016). These differences in crystallographic orientation can induce additional local internal stresses that can play a role in strengthening properties and explain the properties obtained in this study.

Figures 3a,b shows the microstructure after loading in the columnar and equiaxed regions, respectively. The corresponding inserts show OM micrographs obtained at low magnification.
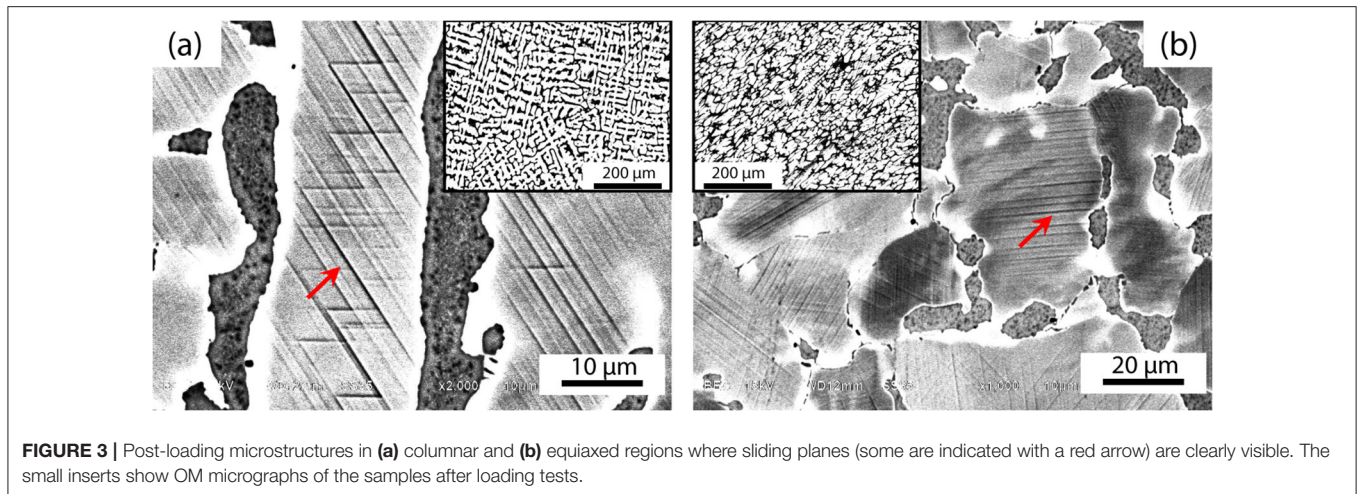
FIGURE 3 | Post-loading microstructures in **(a)** columnar and **(b)** equiaxed regions where sliding planes (some are indicated with a red arrow) are clearly visible. The small inserts show OM micrographs of the samples after loading tests.

Two observations can be made from this figure. The first one concerns the slipping planes that can be observed in both figures but in the fcc phase only. It means that most of the strain is solely accommodated by the fcc phase. A second observation is related to the orientation anisotropy inherent to columnar dendritic structures: the sliding planes in **Figure 3a** all have the same orientation, because all the dendrites arms are oriented along the <100> direction. The number of slip systems is thus limited in this type of microstructure, but also constrained by the interdendritic bcc/B2 phases. This lead to this "stair-like" slipping plane visible in the figure. In **Figure 3b**, the equiaxed grains which have a random orientation show, per grain, one, sometimes two sliding planes of different crystallographic orientation. The observable slip planes thus have a different orientation in each grain. The macroscopic consequence of the difference between columnar and equiaxed zone can be seen in the inserts in **Figures 3a,b**: while the columnar zone does not seem very different from the initial one, the equiaxed microstructure is visibly deformed after the compression test. For the samples with directionally solidified structure tested along the <001> crystallographic orientation, eight slip systems can theoretically be activated if the uniaxial applied stress is larger than CRSS/m, CRSS being the critical resolved shear stress and m the Schmid factor, which is about 0.40 in this case. This large number of activated system is expected to lead to a strong hardening and a limited plastic deformation (Meyers and Chawla, 2008). On the other hand in the samples with an equiaxed structure, each grain with a random orientation will tend to deform plastically according the same relation CRSS/m. However the number of activated slip system is more likely to be limited to 1 (ex: grain oriented along the <123> direction or <153> direction), 2 (ex: grain oriented along <112> direction), 4 (ex: grain oriented along <101> direction), etc., with values of the Schmid factor larger than 0.4. The important number of randomly oriented equiaxed grains ($6.4 \ 10^7$ grains/cm^3 for a grain size of 25 μm) is favorable for the plastic deformation through activation of single slip system compared to the columnar

microstructure. The highest strength and lowest ductility of directionally solidified samples thus comes from the interaction between different slip systems in the fcc phase compared to samples with an equiaxed structure. It is remarkable that no slip system can be observed in the B2 phases suggesting that this phase play the role of reinforcement in this alloy. Further analyses should be carry on to study thoroughly the interaction between both face-centered, disordered and ordered body-centered cubic phases.

4. CONCLUSIONS

The influence of the solidification microstructure on mechanical response of $Al_{0.8}CrCuFeNi_2$ alloy containing fcc and bcc/B2 phases was investigated. Both microstructures contain the same amount of bcc/B2 phases in the interdendritic region. The following conclusions can be drawn:

- When tested under uniaxial compression mode with the loading axis parallel to the direction of solidification, the columnar microstructure, with a preferred orientation of the fcc phase toward the <100> direction exhibits higher mechanical properties than the equiaxed microstructures with fcc grains randomly oriented.
- From the current observation slip is visible in the fcc phase only, and the superior mechanical properties measured for the oriented microstructure are due to a limited number of slipping plane constrained by the interdendritic bcc/B2 region.

DATA AVAILABILITY STATEMENT

The raw data supporting the conclusions of this article will be made available by the authors, without undue reservation.

AUTHOR CONTRIBUTIONS

JZ contributed conception, design of the study, and wrote the first draft of the manuscript. JZ and EF wrote sections of the

manuscript. All authors contributed to manuscript revision, read and approved the submitted version.

REFERENCES

Borkar, T., Gwalani, B., Choudhuri, D., Mikler, C., Yannetta, C., Chen, X., et al. (2016). A combinatorial assessment of $Al_xCrCuFeNi_2$ (0< x <1.5) complex concentrated alloys: microstructure, microhardness, and magnetic properties. *Acta Mater.* 116, 63–76. doi: 10.1016/j.actamat.2016.06.025

Cantor, B., Chang, I., Knight, P., and Vincent, A. (2004). Microstructural development in equiatomic multicomponent alloys. *Mater. Sci. Eng. A* 375, 213–218. doi: 10.1016/j.msea.2003.10.257

Choudhuri, D., Gwalani, B., Gorsse, S., Mikler, C., Ramanujan, R., Gibson, M., et al. (2017). Change in the primary solidification phase from fcc to bcc-based b2 in high entropy or complex concentrated alloys. *Scripta Mater.* 127, 186–190. doi: 10.1016/j.scriptamat.2016.09.023

Gludovatz, B., Hohenwarter, A., Catoor, D., Chang, E. H., George, E. P., and Ritchie, R. O. (2014). A fracture-resistant high-entropy alloy for cryogenic applications. *Science* 345, 1153–1158. doi: 10.1126/science.1254581

Guo, L., Wu, W., Ni, S., Wang, Z., and Song, M. (2017). Effects of annealing on the microstructural evolution and phase transition in an $AlCrCuFeNi_2$ high-entropy alloy. *Micron* 101, 69–77. doi: 10.1016/j.micron.2017.06.007

Guo, S., Ng, C., and Liu, C. T. (2013). Anomalous solidification microstructures in Co-free $Al_xCrCuFeNi_2$ high-entropy alloys. *J. Alloys Compd.* 557, 77–81. doi: 10.1016/j.jallcom.2013.01.007

Meyers, M. A., and Chawla, K. K. (2008). *Mechanical Behavior of Materials*. Cambridge, UK: Cambridge University Press.

Tang, Z., Gao, M. C., Diao, H., Yang, T., Liu, J., Zuo, T., et al. (2013). Aluminum alloying effects on lattice types, microstructures, and mechanical behavior of high-entropy alloys systems. *JOM* 65, 1848–1858. doi: 10.1007/s11837-013-0776-z

Versnyder, F. I., and Shank, M. (1970). The development of columnar grain and single crystal high temperature materials through directional solidification. *Mater. Sci. Eng.* 6, 213–247. doi: 10.1016/0025-5416(70)90050-9

Yeh, J.-W., Chen, S.-K., Lin, S.-J., Gan, J.-Y., Chin, T.-S., Shun, T.-T., et al. (2004). Nanostructured high-entropy alloys with multiple principal elements: novel alloy design concepts and outcomes. *Adv. Eng. Mater.* 6, 299–303. doi: 10.1002/adem.200300567